Korean J. Chem. Eng., 35(9), 1844-1853 (2018)
DOI: 10.1007/s11814-018-0096-7

pISSN: 0256-1115
eISSN: 1975-7220

Synthesis and characterization of CMC/MMT nanocomposite for Cu^{2+} sequestration in wastewater treatment

Hany Fathy Heiba*,†, A. A. Taha, Alaa R. Mostafa***, Laila A. Mohamed*, and Mamdouh A. Fahmy***

*Marine Chemistry Department, Environmental Division, National Institute of Oceanography and Fisheries (NIOF), Alexandria, Egypt
**Department of Chemistry, Faculty of Science, Alexandria University, Alexandria, Egypt
***Department of Environmental Sciences, Faculty of Science, Alexandria University, Alexandria, Egypt
(*Received 7 May 2018 • accepted 4 June 2018*)

Abstract−Organic–inorganic hybrid nanocomposites are promising materials for remediation of pollutants from wastewater, as they exhibit the unique characteristics of both inorganic and organic materials. In this study, carboxymethyl cellulose/montmorillonite Nanocomposite (CMC/MMT-NC) was prepared and applied for Cu^{2+} sequestration. CMC/MMT-NC was characterized by FTIR and SEM before and after the sequestration process, indicating fundamental changes in surface morphology after treatment experiments. The parameters affecting the process such as pH, contact time, CMC/MMT-NC mass, Cu^{2+} concentration and temperature were experimentally adjusted. Statistical regression variables (R^2, RMSE, RSS, F-Value and P-Value) were calculated to predict the best-applied isotherm, kinetic and thermodynamic modeling. Freundlich isotherm model successfully described the equilibrium data, which implies a multilayer adsorption process. Kinetic results were well fitted to pseudo-second-order kinetic model. Intraparticle diffusion (IPD) model showed the control of the boundary layer moreover, IPD model cannot be accepted as the only rate-determining step. The apparent activation energy (Ea) was 35.65 kJ/mol, which revealed a physisorption process. The thermodynamic study in means of ΔG^0, ΔH^0, and ΔS^0 demonstrated the feasibility, spontaneity and exothermicity of Cu^{2+} sequestration. Application study confirmed the efficiency of CMC/MMT nanocomposite to remediate Cu^{2+} from synthetic and natural polluted seawater.

Keywords: CMC/MMT-NC, Regression Analysis, Cu^{2+} Sequestration, Kinetics, Isotherm, Thermodynamics

INTRODUCTION

The rapid development of industries such as metal plating, mining, tanneries, batteries, electronics, petrochemical, textile, etc. has contributed to excessive metal concentrations through direct or indirect discharge into the environment, mainly in developing countries [1]. Thus, metal pollution has become an essential focus environmentally. Although some heavy metals are essential to living organisms at low concentrations, they become toxic at elevated concentrations. Heavy metals are the worst group of the environmental pollutants [2] due to their toxicity, non-degradable nature, and tendency to bioaccumulate [1]. Copper is extensively used in industries such as electrical, electronics, building construction, industrial machines and equipment fabrication. The available amount of copper may not be guaranteed due to its growing demand and shrinking resources [3]. Copper is an essential trace metal required in small amounts (1-1.5 mg/day) by humans, animals, fish and shellfish for haemoglobin synthesis, metabolism purposes and enzyme functioning. However, copper can be harmful when it exceeds the tolerance limit [2]. Poisoning with Cu causes different symptoms and diseases like a headache, hair loss, heartbeats, liver malfunction, kidney damage, anemia and intestinal problems [4]. Thus, it is necessary to develop an inexpensive, efficient and environmental green approach with high selectivity capacity towards Cu^{2+} [5].

Conventional methods such as chemical precipitation, coagulation, ion exchange and membrane technology have been generally applied for the treatment of copper contaminated wastewater. However, each of these methods has its own limitations [6]. Adsorption is considered as the most conventional method for heavy metals removal because of its simplicity and cost effectiveness [4].

Clay minerals have well-recognized adsorption capabilities in addition to the extensive use in industrial, technological, and environmental applications. For example, montmorillonite (MMT) has been utilized in removal of toxic metals due to its availability, high mechanical stability, good swelling ability, large specific surface area and high cation exchange capacity [7]. Previous studies indicated that the addition of organic modifier (e.g., biopolymer) can greatly affect the structure and adsorptive properties of MMT [8]. Biopolymers have an excellent biocompatibility, biodegradability and non-toxicity. However, they have some limitations such as poor mechanical strength and lack of reusability [9]. Therefore, clays such as MMT can be used as a matrix to overcome these limitations. Biopolymer-based nanocomposite combines the advantages of both matrix and polymer: like the large surface area to volume ratio, the en-

†To whom correspondence should be addressed.
E-mail: hanyheiba@gmail.com, hf.heiba@niof.sci.eg
Copyright by The Korean Institute of Chemical Engineers.

Table 1. Experimental conditions for the adsorption experiments

Studied parameter	Time (min)	pH	C_0 (mg/L)	Adsorbent mass (g)	Agitation speed (rpm)	Temperature (K)
Time (min)	1-60	5	10	0.1	100	298
pH	60	2-7	10	0.1	100	298
Cu^{2+} concentration, C_0 (mg/L)	60	5	5-20	0.1	100	298
Adsorbent mass (g)	60	5	10	0.05-0.2	100	298
Temperature (K)	60	5	10	0.1	100	293-328

hanced chemical reactivity, the high mechanical stability and the ease of regeneration [10]. Cellulose derivatives like carboxymethyl cellulose (CMC) possess polar groups like carboxymethyl groups (-CH_2COOH) which increase the chelation ability and solubility in water, and consequently CMC can be employed as modifying polymer in nanocomposite synthesis [11]. Due to their unique characteristics, nanocomposites have received a high interest in removal of heavy metals [5] and organic pollutants [12-14].

We synthesized a hybrid nanocomposite utilizing MMT and CMC; hence, it can express the unique characteristics of both the inorganic and organic materials. The objectives of the present study were: (1) Preparation and structural characterization of CMC/MMT-NC, then investigation of its potential toward Cu^{2+} removal; (2) Optimization of the experimental factors such as pH, contact time, nanocomposite dosage, temperature and metal ion concentration; (3) Statistical analysis of the adsorption isotherm, kinetics, mechanism and thermodynamic; and (4) Evaluation of the CMC/MMT-NC competence to remove heavy metal ions from polluted seawater.

MATERIALS AND METHODS

1. Preparation of CMC/MMT-NC

First, a CMC solution was prepared by dissolving 1.0 g of CMC (Sigma-Aldrich) powder in 100 mL (1.0% w/v of distilled H_2O) in a round flask, which was fitted with an argon gas inlet in a water bath (Thermo) at 60 °C and continuous stirring [11]. Second, 1.00 g of Montmorillonite (Obtained from Egyptian Bentonite and Derivatives Co.) was added in 100 mL of deionized water and magnetically stirred, at 60 °C for 15 min. Then, the CMC solution was added to the montmorillonite suspension (in 4 : 1 ratio) and stirred at 800 rpm under 60 °C for 5 h. The mixture was poured onto a clean glass plate and the solvent was evaporated in an oven at 50 °C for 12 h. Finally, the resulting hybrid CMC/MMT-NC was gently removed from the glass plates and conditioned in a desiccator for experimental work.

2. Instrumentation

The surface morphology of the synthesized CMC/MMT-NC hybrid composite was characterized using SEM with a Jeol-JSM-5300 apparatus. The surface functional groups were screened by FT-IR (PerkinElmer Spectrum BX) in the range of 400-4,000 cm^{-1}. The chemical analysis was by means of XRF - (ALR 9400). The pH values were adjusted using pH meter (JENWAY-3505). Sartorius digital balance was used for weighing. Thermo orbital shaker (Thermo 436 - HEPA Filter) was used for shaking in during batch experiments. Copper concentration was measured using an atomic absorption spectrophotometer (Shimadzu AAS-6800).

3. Batch Adsorption Experiments

Standard stock solution of 1,000 mg/L $Cu(NO_3)_2$ was purchased from MERK-Germany; the specified Cu^{2+} concentrations were prepared by dilution of the stock solutions immediately before use and deionized water was used throughout the experiments. The required pH of each solution was adjusted by adding 0.1 M NaOH (Loba-Chemie) or 0.1 M HNO_3 (Analar-R). The metal solution was added to certain weights of the CMC/MMT-NC composite and agitated. Finally, the remaining unadsorbed copper ion traces were determined by atomic absorption spectrophotometer. The adsorption parameters were studied under the conditions listed in Table 1.

4. Data Analysis

Removal efficiency (% removal) was calculated from Eq. (1), while the equilibrium amount (mg/g) of Cu^{2+} ions adsorbed onto CMC/MMT-NC hybrid composite (metal uptake capacity) was calculated by difference using Eq. (2):

$$\text{Adsorption efficiency}\,(\%) = \frac{C_o - C_e}{C_o} \times 100 \tag{1}$$

The adsorption capacity (q_t) "the amount of copper adsorbed per gram adsorbent (mg/g)" was calculated using Eq. (2);

$$q_t = \frac{(C_o - C_t)V}{m} \tag{2}$$

where C_o, C_e and C_t represent the copper concentration (mg/L) at the beginning, equilibrium and at time (t), respectively. V is the solution volume in liter (L) and m is the adsorbent weight in grams (g). The data obtained were applied to the isotherm, kinetics and thermodynamic models.

5. Statistical Regression Analysis

The relations and comparisons between data output were analyzed statistically using Origin-8 ANOVA software through calculation of statistical regression variables like R^2, root mean square error (RMSE=SD), residual sum of squares (RSS), F-Value, P-Value (Prob>F).

RESULTS AND DISCUSSION

1. Characterization of CMC/MMT-NC

1-1. FTIR Spectral Analysis

FTIR spectra for CMC/MMT-NC before and after the remediation process are included in Fig. 1. The absorption band at 3,400-3,850 cm^{-1} is ascribed to the stretching vibration of the lattice OH and OH of the physically adsorbed water. The peaks at 2,862 and 2,924 cm^{-1} are due to the C-H stretching vibration of the CMC. The

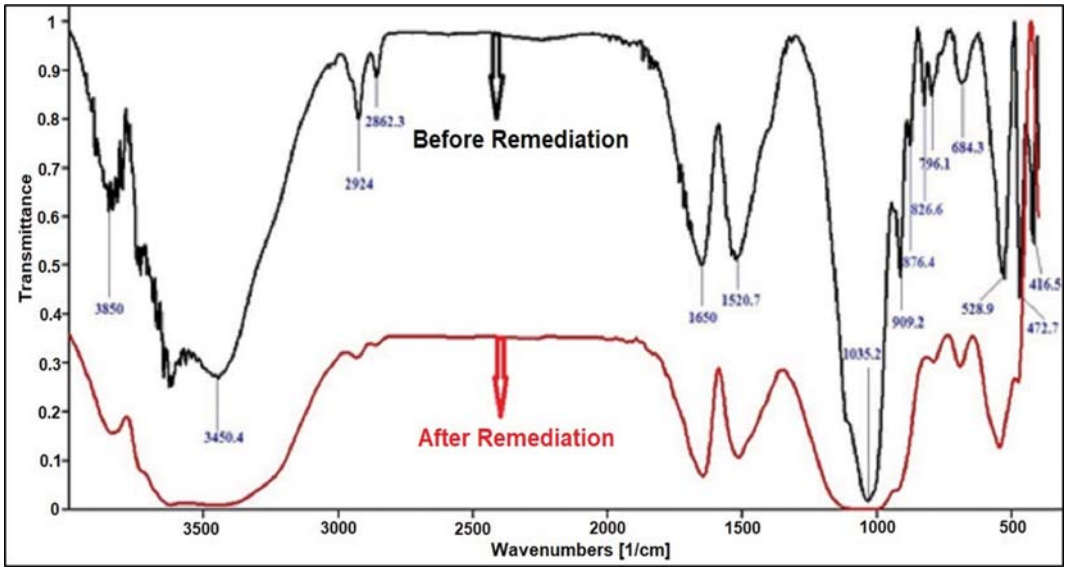

Fig. 1. FTIR spectra for sequestration of Cu^{2+} by CMC/MMT hybrid composite before and after sequestration.

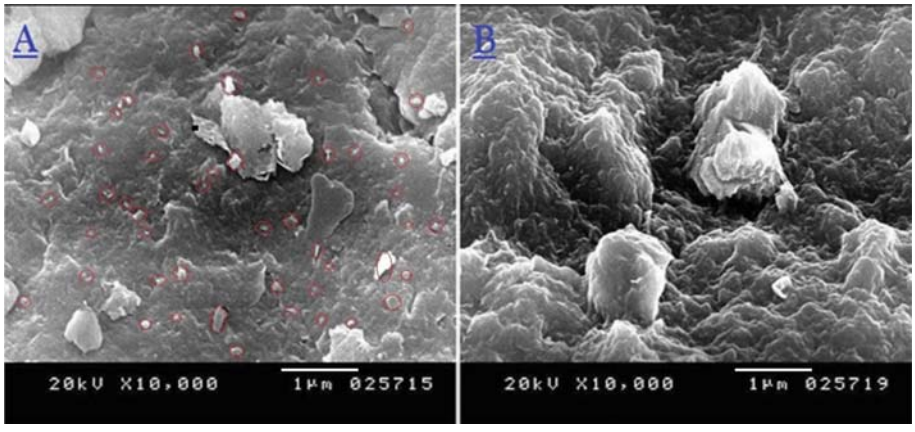

Fig. 2. SEM micrograph for sequestration of Cu^{2+} onto CMC/MMT-NC [A- before sequestration, B- after sequestration].

band around 1,650 cm^{-1} is attributed to the stretching vibration of the carbonyl (C=O) in CMC. The peaks at 1,520 cm^{-1} were due to the characteristic stretching vibrational bands of O-Si-O in MMT. The strong band at 1,035 cm^{-1} is caused by both stretching frequencies of Si-O-Si (in MMT) and C-O-C (in CMC). The three bending vibrations at 909 cm^{-1}, 876 cm^{-1} and 826 cm^{-1} are considered for (Al-Al-OH), (Al-Fe-OH) and (Al-Mg-OH), respectively, which were due to binding of the hydroxyl group with Al^{+3} cations in MMT. Bands around (416-796) cm^{-1} in the stretching mode result from the Si-O-Al and Si-O-Mg stretching frequency, and SiO bending frequencies. After remediation experiments, the reaction of the copper ions with the surface functional groups was pronounced. The intensity of most peaks was reduced and shifted like the peaks of C-H, C=O, SiO, O-Si-O, C-O-C groups. In addition, some bands disappeared (e.g., bands of Si-O-Al, Si-O-Mg stretching vibration, and SiO bending frequencies); moreover, the deep band at 1,035 cm^{-1} was widened. These changes are the result of copper ions attachment to the clay lattice. Furthermore, there was an increase in the broadness of the hydroxyl group band [15].

1-2. SEM Analysis (Morphology Characteristics)

SEM micrographs of CMC/MMT-NC composite before and after Cu^{2+} loading are shown in Fig. 2. It is clear that CMC/MMT-NC surface is heterogeneous, exhibiting irregularity and roughness, which promotes metal adsorption. The Cu-laden CMC/MMT-NC showed significant morphological changes with evidence of an increase in irregularity and roughness, authenticating the adsorption of Cu^{2+} ions and surface shielding with copper film which is formed due to binding of Cu^{2+} ions to CMC polymer, causing relaxation of the composite texture. In addition, the MMT contains exchangeable cations such as Ca^{2+}, K^{1+}, Mg^{2+}, and Na^{1+} which can be replaced Cu^{2+} [16].

2. Operating Parameters

2-1. Adsorption Profile as a Function of pH

Solution pH can greatly affect the surface charge of CMC/MMT-NC, ionization degree and Cu^{2+} species. The pH effect is remarkedly pronounced when both the adsorbent and adsorbate have strong intermolecular interactions (i.e., H-bond, ion-dipole, or dipole-dipole forces) [11]. pH effect was investigated within pH range (2-

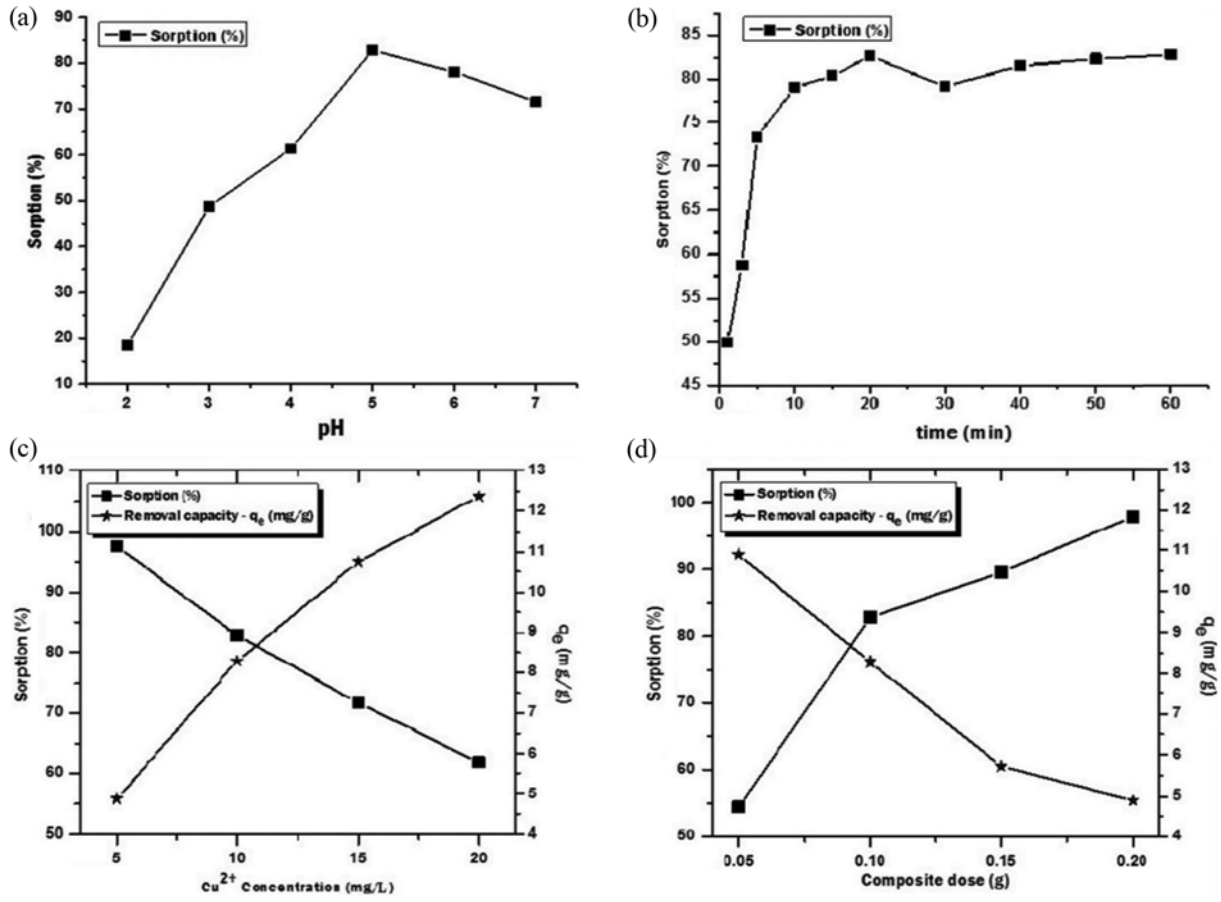

Fig. 3. Effect of operating parameters on Cu^{2+} sequestration (a) Effect of pH. (b) Effect of contact time. (c) Effect of Cu^{2+} concentration on sorption % and sorption capacity. (d) Effect of CMC/MMT-NC dosage mass on sorption % and sorption capacity.

7), while other variables were kept constant. Fig. 3(a) shows that % removal was very low as about 18.5% at pH 2 then gradually increased until peaking at pH 5 as about 82.8%. However, beyond pH 5 the sorption % decreased, this can be illustrated upon the magnitude of the surface charge. It is possible to suggest that at lower pH, the composite surface is covered with hydronium ions (H^+) which compete with copper ions and prevent them from approaching the surface binding sites due to electrostatic repulsive forces. Increasing the pH resulted in a decrease in the surface charge density, and so the repulsive forces between the positively charged metal ions and the composite surface was reduced, causing a higher removal %. At pH 6, the sequestration capacity was slightly diminished due to the partial hydrolysis of Cu^{2+} in the form of $Cu(OH)^+$ and $Cu(OH)_2$ in large quantities, which would be adsorbed at a lower extent compared to free Cu^{2+} ions [17]. A study beyond pH 7.0 was not possible because of the appearance of insoluble copper-hydroxide-precipitate in the solution. The results showed that pH 5 was the optimal solution pH for removal of copper ions using CMC/MMT-NC.

2-2. Effect of Shaking Time

Determination of the equilibrium contact time is an important parameter not only for the adsorption process, but also for the operational cost. Fig. 3(b) indicates that increasing the contact time resulted in a higher % removal of Cu^{2+} until plateauing at 40 min. The adsorption process was fast at the beginning stages because of the availability of vacant binding sites on CMC/MMT-NC composite as the time passed, these active sites became more reacted and covered with Cu^{2+} ions, which restricted further binding of Cu^{2+}. The short equilibrium time (40 min) provides an economic advantage for the large-scale application because it means a shorter agitation period (less energy consumption) and hence, results in a reduction of operational costs [11].

2-3. Influence of Cu^{2+} Concentration

The influence of the initial copper ion concentration is presented in Fig. 3(c). It is obvious that the metal concentration had a considerable effect on the sorption % and the adsorption capacity, whereas, with the increase in copper concentration, the sorption % declined but the adsorption capacity increased. The decrease in % removal can be explained by the competition between copper ions to bind to the available active sites at higher Cu^{2+} concentrations. On the other hand, the increase in the adsorption capacity at higher Cu^{2+} concentrations can be attributed to the increase in driving force, which defeats the mass transfer resistance of Cu^{2+} ions between the aqueous and solid phase. This results in employment of all active sites and the internal pores in the adsorption process and so a higher q_e is obtained [18].

2-4. Effect of CMC/MMT-NC Mass

Fig. 3(d) displays the effect of the nanocomposite mass on the

corresponding uptake percentage and the equilibrium adsorption capacity. With increasing the CMC/MMT-NC dosage from 0.05 to 0.2 g, the removal % increased from 54.47 to 97.89%; this increase was because at a fixed Cu^{2+} concentration, the increase of adsorbent mass leads to a greater surface area and that augments the number of active sites available for binding with copper. However, the adsorption capacity (q_e) decreased with the increase in the composite dosage due to the increase of unsaturation of active sites "high (active sites/metal ions) ratio"; in addition the higher dosage resulted in the agglomeration of the nanocomposite particles and so increased the diffusional path length; hence, the adsorption capacity dramatically decreased [19].

3. Statistical Regression Analysis for Isothermal, Kinetics and Thermodynamics

We used statistical regression analysis (using ANOVA, Origin 8 program) to examine and compare the best applied isotherm, kinetics and thermodynamic models. The used statistical regression variables were as follows:

i) Coefficient of Determination (R^2): represents how well the model fits for all the data Eq. (3)

$$R^2 = \frac{SS_{Regression}}{SS_{Total}} \tag{3}$$

where SS Regression is the sum squared regression error and SS total is sum squared total error

ii) Root Mean Square Error (RMSE=SD): the standard deviation of the residuals, which indicates the differences between predicted values and observed values Eq. (4):

$$RMSE = \sqrt{\frac{\sum_{i=1}^{N}(p_i - o_i)^2}{N}} \tag{4}$$

where N is the sample size and (pi-oi) ids the difference between predicted and observed vales

iii) Residual Sum of Squares (RSS): RSS determines if a statistical model can fit the data well. It is a measure of the total variation between the obtained data and the predicted values Eq. (5)

$$RSS = \sum_{i=1}^{N}(y_i - \tilde{y}_i)^2 \tag{5}$$

iv) F-Value: the ratio of two mean squares and it is computed by dividing the mean square of fitted model by the mean square of error Eq. (6)

$$F = \frac{(RSS_1 - RSS_2)/(p_2 - p_1)}{RSS_2/(n - p_2 - 1)} \tag{6}$$

where p; is the parameter of each model. The larger F Value significantly predict the best model [20].

v) P-Value (Prob > F): The p-value represents the smallest level of significance at which the null hypothesis would be rejected; thus the smaller p-value, the most acceptable model [21].

3-1. Isothermal Studies

Adsorption isotherms represents a functional expression which correlates the amount of the adsorbed adsorbate per unit mass of the adsorbent with the remaining adsorbate concentration in the bulk solution at a constant temperature and under equilibrium conditions [10]. Langmuir and Freundlich isotherm models were applied in their linear form to describe the sorption equilibrium of copper ions. Langmuir isotherm assumes monolayer adsorption and the chemical binding of the adsorbate to the adsorbent surface where all sites on the surface have an equal affinity for the metal ions. The Langmuir model is represented by Eq. (7).

$$\frac{C_e}{q_e} = \frac{1}{q_m b} + \frac{C_e}{q_m} \tag{7}$$

C_e represents the equilibrium concentration (mg/L), q_e is the adsorption capacity ($mg_{(metal)}/g_{(adsorbent)}$) in at equilibrium, q_m is the Langmuir adsorption capacity which is the quantity of the metal necessary to produce a monolayer on the surface of the sorbent, b is the Langmuir equilibrium constant (L/mg). Langmuir plot is presented in Fig. 4(a) and the related isothermal parameters are in Table 2.

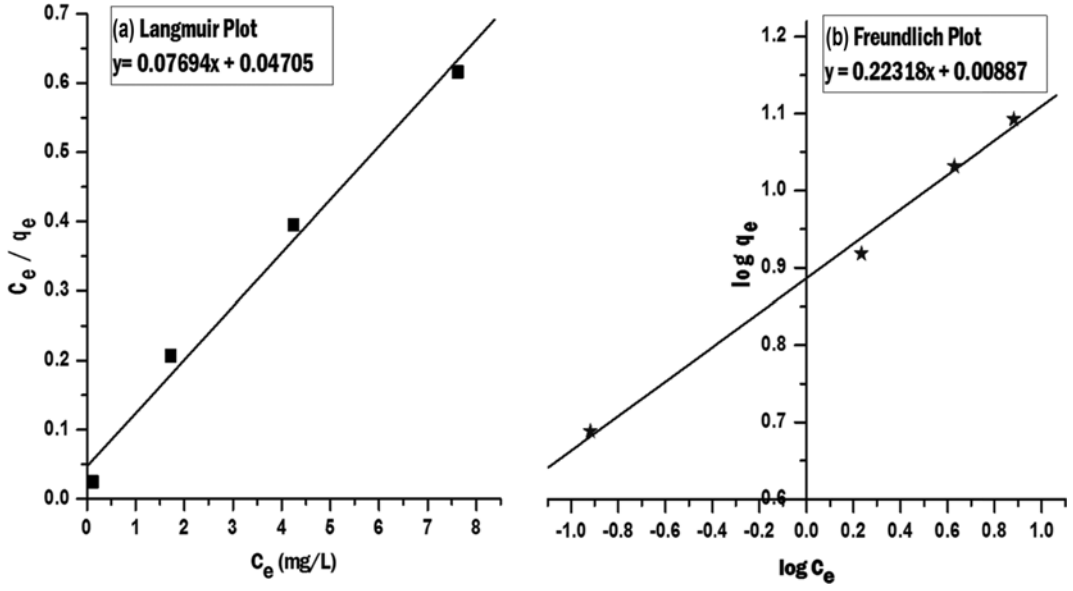

Fig. 4. Isothermal plots for adsorption of Cu^{2+} onto CMC/MMT-NC ((a) Langmuir plot, (b) Freundlich model).

Table 2. Isothermal parameters for adsorption of Cu^{2+} onto CMC/MMT composite

Langmuir isotherm parameters								
q_m (mg/g)	b (L/mg)	R_L	RMSE (SD)	RSS	F Value	Prob>F	R^2	DF
12.997	1.635	C_o=5 mg·L^{-1} 0.109 C_o=10 mg·L^{-1} 0.058 C_o=15 mg·L^{-1} 0.039 C_o=20 mg·L^{-1} 0.030	0.0079	0.0159	149.7957	0.0066	0.9802	3
Freundlich isotherm parameters								
K_F (mg/g)		1/n	RMSE (SD)	RSS	F Value	Prob>F	R^2	DF
7.701		0.223	0.0003	0.0006	327.6150	0.0030	0.9909	3

The obtained high values of R^2 (>0.98) reveal well-fitting to the Langmuir model. The Langmuir maximum sorption capacity of Cu^{2+} by CMC/MMT-NC is 12.99 mg/g, which highlights the potential of the nanocomposite under the studied conditions. The separation factor R_L given by Eq. (8) is a characteristic index of the Langmuir model, which is usually applied to assess the adsorption favorability thermodynamically: when R_L>1 this implies an unfavorable adsorption; when R_L=1, means a linear adsorption; when 0<R_L<1, adsorption is favorable; when R_L=0, it is an irreversible process [22].

$$R_L = \frac{1}{1+bC_o} \tag{8}$$

The obtained R_L values ranged from 0.029 to 0.109, implying that Cu^{2+} sorption was favorable. R_L values are inversely proportional to the initial concentration (Table 2), indicating that the sorption can be further increased with the increase in initial concentrations.

Freundlich isotherm describes a multilayer heterogeneous adsorption on the surface and it is given by Eq. (9).

$$\log q_e = \log K_F + \frac{1}{n}\log C_e \tag{9}$$

where, K_F is the Freundlich constant which is a measure of the adsorption capacity and n is the adsorption intensity. Fig. 4(b) shows the Freundlich plot, and its related coefficients are presented in Table 3. R^2 and 1/n values confirmed the applicability of Freundlich model where the obtained values (R^2>0.99 and 1/n<1) which further reflect the high affinity between Cu^{2+} and CMC/MMT-NC [23].

However, both Langmuir and Freundlich show good R^2 fitting; on the basis of regression coefficients (smaller RMSE, smaller RSS value, higher F-Value, smaller p-value) the experimental data is best followed by Freundlich isotherm rather than both, which indicates that multilayer (heterogeneous) adsorption was involved in the sequestration process [7].

3-2. Kinetic Studies

Kinetic studies give a valuable insight to the sequestration process through depicting the process at the solid-solution interface. Two kinetic models, pseudo-first-order (PFO) and pseudo-second-order (PSO), were selected in this study to investigate the adsorption kinetics [24]. The PFO kinetic model is expressed in Eq. (10).

$$\ln(q_e - q_t) = \ln q_e - k_1 t \tag{10}$$

where q_e and q_t are the mass of Cu^{2+} (mg) adsorbed on CMC/MMT-NC (g) at the equilibrium and at time t, respectively; k_1 is the PFO rate constant (min^{-1}).

The PSO kinetic model is given in the linear form in Eq. (11)

$$\frac{t}{q_t} = \frac{1}{k_2 q_e^2} + \frac{t}{q_e} \tag{11}$$

where, k_2 is the PSO rate constant (g·$mg^{-1}min^{-1}$). The graphical plots for both PFO and PSO kinetic models are shown in Fig. 5(a)

Table 3. Kinetic parameters for sequestration of Cu^{2+} onto CMC/MMT

	Pseudo-first-order kinetics				Pseudo-second-order kinetics			
C_o (mg/L)	5	10	15	20	5	10	15	20
$q_{e,exp.}$ (mg/g)	**4.879**	**8.284**	**10.753**	**12.375**	**4.879**	**8.284**	**10.753**	**12.375**
$q_{e,cal.}$ (mg/g)	**0.601**	**1.201**	**1.562**	**4.349**	**4.947**	**8.357**	**10.841**	**12.736**
k*	0.075	0.069	0.061	0.076	0.34	0.15	0.114	0.048
R^2	0.218	0.416	0.469	0.944	0.999	0.999	0.999	0.999
RMSE	3.91589	1.71935	1.11075	0.09452	0.00623	0.00279	0.00152	0.00165
RSS	15.66356	12.03543	7.77522	0.56714	0.04982	0.02228	0.01216	0.01322
F Value	2.39625	6.70557	8.07656	118.3541	25490.4	19969.61	21735.2	14488.99
Prob>F	0.19654	0.03597	0.02498	$3.58E^{-05}$	$2.66E^{-15}$	$6.99E^{-15}$	$5.00E^{-15}$	$2.53E^{-14}$
DF	5	8	8	7	9	9	9	9

k*: "k_1 (min^{-1}) in case of Pseudo-first-order kinetics and k_2 (g $mg^{-1}min^{-1}$) in case of Pseudo-second-order kinetics"

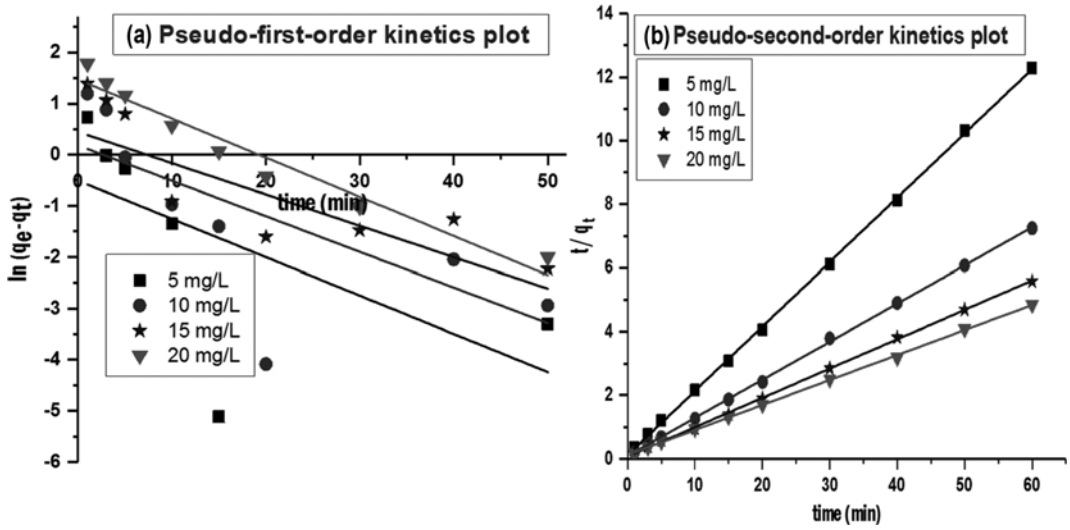

Fig. 5. Kinetics plots for adsorption of Cu^{2+} onto CMC/MMT composite ((a) Pseudo-first-plot, (b) Pseudo-second-model).

& (b), respectively, and the kinetic constants are listed in Table 3. The results show that PFO kinetic model displays very poor linearity and does not cover the full range of the contact time (it was suitable only for the initial 50 min), and the calculated q_e is far from the experimental q_e. On the other hand, the PSO plot (Fig. 5(b)) is applicable over the whole range of contact time with an excellent linearity (R^2>0.99), and the calculated q_e is very close to the experimental q_e. Moreover, in PSO model the rate constant k_2 showed a logic decreasing trend with the increase in the initial concentration due to the coverage of the binding sites but in PFO; no trend was observed for the rate constant k_1. The comparison of the statistical variables (R^2, RMSE, RSS, F-value and P-value) supported the PSO model hypothesis. Therefore, it is reasonable to conclude that sequestration of Cu^{2+} on CMC/MMT-NC follows the PSO model [15]. The failure of the PFO model to describe the kinetic data could be because of the limitations of boundary layer controlling the sorption process (as discussed in the next section). The applicable PSO model cannot identify the diffusion mechanism, so the Weber-Morris intraparticle diffusion model was used for a further investigation of the kinetic data [25]. IPD model elucidates the diffusion mechanism through the influence of mass transfer resistance on the binding of Cu^{2+} to CMC/MMT-NC; the model is represented in Eq. (12):

$$q_t = k_{id} t^{0.5} + C \quad (12)$$

where k_d is the IPD rate constant (mg/gmin$^{1/2}$) and C is the intercept which describes the effect of the boundary layer. Larger C value means a higher contribution of the surface sorption in the rate-determining step. If the Weber-Morris plot of q_t versus $t^{0.5}$ gives a straight line that passes through the origin, then the IPD is the only rate-determining step. However, the obtained plots in Fig. 6 deviate from linearity, presenting multi-linear sections. The deviation from the origin maybe due to the difference in the mass transfer rate during the initial and final stages of adsorption. This indicates that there is some degree of boundary layer control and the IPD was not only the rate-controlling step in Cu^{2+} sequestration by CMC/MMT-NC [26]. From Table 4, it obvious that as times increases, the IPD rate constant decreases (ki_{d1}>k_{id2}>ki_{d3}) due to the increase in boundary layer thickness (C) with time (C_1<C_2<C_3), so the boundary (surface) diffusion becomes more effective as a rate-limiting step [27].

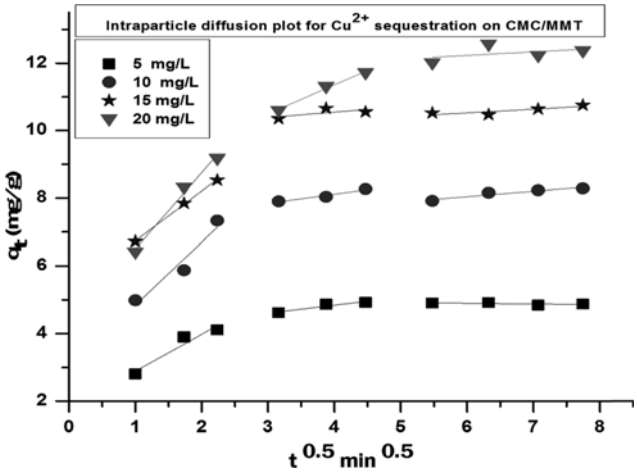

Fig. 6. IPD diffusion model for Cu^{2+} sequestration by CMC/MMT-NC (where; The three sections in the plot represents: (1) Transport of Cu^{2+} from the bulk solution to the external surface of CMC/MMT (Film diffusion). (2) Intraparticle or pore diffusion, where Cu^{2+} move into the interior pores; and, (3) Equilibrium attained).

3-3. Activation Energy for Sequestration

The apparent activation energy (Ea) was calculated using Arrhenius equation [28] given in Eq. (13)

$$\ln k_2 = \ln A - \frac{E_a}{RT} \quad (13)$$

where K_2 is the PSO kinetic rate calculated at different temperatures (293-308 K) using the PSO kinetic model, R is the universal gas constant (8.314 J/mole K) and T is the absolute temperature (K).

Table 4. Intraparticle diffusion parameters for sequestration of Cu^{2+} onto CMC/MMT

	C_0 (mg/L)	K_1 (mg g^{-1} min$^{-0.5}$)	C_1	R_1^2	RMSE (SD)	RSS	F value	Prob>F	DF
First linear section	5	1.092	1.795	0.932	0.259	0.067	13.694	0.168	2
	10	1.848	3.005	0.941	0.407	0.166	15.889	0.156	2
	15	1.472	5.265	0.999	0.044	0.002	868.507	0.022	2
	20	2.255	4.245	0.988	0.220	0.048	81.263	0.070	2
	C_0 (mg/L)	K_2 (mg g^{-1} min$^{-0.5}$)	C_2	R_2^2	RMSE (SD)	RSS	F value	Prob>F	DF
Second linear section	5	0.236	3.901	0.904	0.071	0.005	9.455	0.200	2
	10	0.273	7.024	0.958	0.053	0.003	22.633	0.132	2
	15	0.161	9.903	0.453	0.164	0.027	0.830	0.530	2
	20	0.854	7.939	0.990	0.080	0.006	96.982	0.064	2
	C_0 (mg/L)	K_3 (mg g^{-1} min$^{-0.5}$)	C_3	R_3^2	RMSE (SD)	RSS	F value	Prob>F	DF
Third linear section	5	−0.023	5.040	0.413	0.033	0.002	1.409	0.357	3
	10	0.159	7.087	0.908	0.061	0.007	19.779	0.047	3
	15	0.111	9.861	0.733	0.080	0.013	5.479	0.144	3
	20	0.106	11.594	0.197	0.256	0.131	0.490	0.556	3

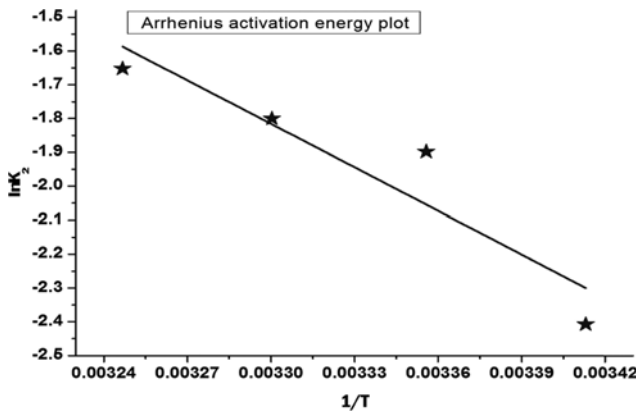

Fig. 7. Arrhenius plot for adsorption of Cu^{2+} onto CMC/MMT-NC.

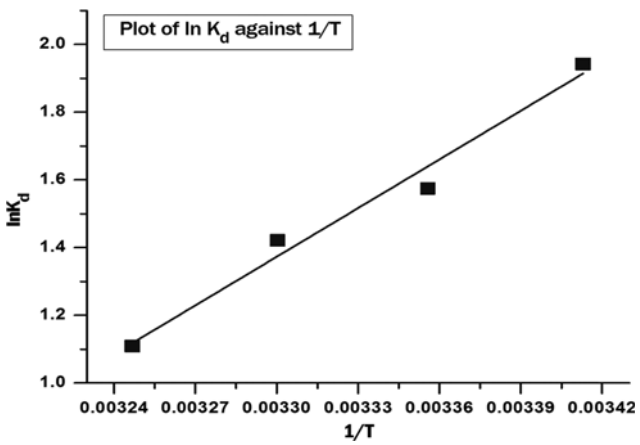

Fig. 8. Plot of ln k_d against 1/T.

E_a values were calculated from the slope of lnk_2 versus 1/T plot (Fig. 7). The obtained E_a value (35.65 kJ/mol) indicates the physisorption of Cu^{2+} onto CMC/MMT-NC, which normally has Ea vales of (5-40 kJ mol^{-1}), while higher activation energy (40-800 kJ mol^{-1}) means a chemisorption process. The resulting E_a value (<42 kJ/mol) also confirms the results of the IPD that the boundary diffusion plays an essential role as a rate-limiting step [29].

3-4. Thermodynamic Analysis

Thermodynamic parameters are important factors to determine the spontaneity degree and energy requirement. The temperature effect on Cu^{2+} adsorption onto CMC/MMT-NC was studied at different temperatures (from 293 to 308 K). Adsorption thermodynamic parameters such as Gibbs energy, ΔG^0 (kJ mol^{-1}), standard entropy change, ΔS^0 (J mol^{-1} K^{-1}) and standard enthalpy change, ΔH^0 (kJ mol^{-1}) were determined using Eq. (14) and (15) [30].

$$\Delta G^0 = -RT\ln K_d \tag{14}$$

$$\ln K_d = \frac{\Delta S^0}{R} - \frac{\Delta H^0}{RT} \tag{15}$$

where K_d is the thermodynamic distribution coefficient and was

Table 5. Thermodynamic constants for sequestration of Cu^{2+} by CMC/MMT

Metal	T (K)	K_d (q_e/c_e)	ΔG^0	ΔH^0	ΔS^0	R^2	RMSE (SD)	RSS	F value	Prob>F	DF
Cu^{2+}	293	6.974	−4.731	−39.844	−0.120	0.980	0.061	0.007	96.286	0.010	3
	298	4.828	−3.901								
	303	4.141	−3.58								
	308	3.031	−2.839								

Table 6. Summary of application study results

	Synthetic seawater	Natural seawater
C_o (Untreated)	10 mg/L	18.66 μg/L
C_e (Treated)	4.62 mg/L	1.45 μg/L
q_e	5.34 mg/L	17.20 μg/g
Sequestration (%)	53.760	92.05

calculated using Eq. (16).

$$K_d = \frac{q_e}{C_e} \quad (16)$$

ΔH^0 and ΔS^0 values were calculated from the slope and intercept of (1/T) against ln K (Fig. 8); the resulting data are presented in Table 5. The statistical regression variables show a good fit, the negative values of ΔG^0 at various temperatures indicate the feasibility of the process and spontaneous nature of the adsorption. However, negativity of ΔG^0 decreases with the increase in temperature, which indicates the sequestration of Cu^{2+} by CMC/MMT-NC composite is unfavorable at elevated temperature [31]. The negative ΔH^0 value emphasizes the exothermic nature of the process. Negative ΔS^0 reveals the stability of the process and the ordered arrangement of Cu^{2+} at the solid-solution interface [17].

4. Application Study on Synthetic and Natural Seawater

The results from the previous optimized experiments were applied to remove Cu^{2+} from synthetic seawater spiked with 10 mg/L Cu^{2+} ions and from natural polluted seawater samples collected from El-mex bay, Alexandria, Egypt. The experiments were done using 60 min agitation time; the pH was adjusted to 5 and 0.1 g CMC/MMT-NC dosage. The results are in Table 6, indicating that the adsorption capacity was diminished from 8.28 mg/g (using deionized water) to 5.34 mg/g (using synthetic seawater) and dramatically deceased to 17.20 μg/g (using polluted natural seawater). This decrease in the adsorption capacity because seawater is a complex matrix containing high concentrations of several mineral ions, such as Na^{1+} (10 g/L), Mg^{2+} (1.2 g/L) and Ca^{2+} (0.4 mg/L) and other compounds which interfere with the Cu^{2+} ions for binding to active sites of CMC/MMT-NC, thereby decreasing the adsorption capacity. However, CMC/MMT-NC exhibits a high removal potential of Cu^{2+} from real seawater (92.05%) with respect to its low initial concentration.

CONCLUSION

We developed a CMC/MMT-NC hybrid composite which has the characteristic features of both CMC and MMT. The prepared composite showed high potential to remove toxic Cu^{2+} from contaminated freshwater, synthetic seawater, and natural seawater. CMC/MMT-NC was characterized using SEM and FTIR before and after removal experiments; the output results showed significant changes in the surface morphology due to binding of Cu^{2+} to the surface-active groups. The operating parameters (pH, contact time, CMC/MMT-NC mass, metal concentration and temperature) were studied and the optimum conditions were determined. Statistical regression analysis revealed that copper remediation followed Freundlich isothermal model, and PSO kinetic model was the suitable model that described the process accurately; the IPD mechanism was not the only the rate-limiting step, but also the boundary layer control is involved in the process. The Arrhenius activation energy (E_a) was 35.65 kJ/mol, which revealed the physisorption nature of the process. Thermodynamic parameters (ΔG^0, ΔH^0 and ΔS^0) showed that Cu^{2+} sequestration was feasible, spontaneous and exothermic. Application studies confirmed that CMC/MMT-NC could eventually be used as an alternative adsorbing material for removal of Cu^{2+} from freshwater, synthetic seawater and natural seawater.

ACKNOWLEDGEMENT

The study was financially supported from National Institute of Oceanography and Fishers (NIOF), Alexandria, Egypt.

REFERENCES

1. S. N. Do Carmo Ramos, A. L. P. Xavier, F. S. Teodoro, L. F. Gil and L. V. A. Gurgel, *Ind. Crop. Prod.*, **79**, 116 (2016).
2. K. Vijayalakshmi, T. Gomathi, S. Latha, T. Hajeeth and P. N. Sudha, *Int. J. Biol. Macromol.*, **82**, 440 (2016).
3. R. Jain, D. Dominic, N. Jordan, E. R. Rene, S. Weiss, E. D. van Hullebusch and P. N. Lens, *Chem. Eng. J.*, **284**, 917 (2016).
4. R. Davarnejad and P. Panahi, *J. Ind. Eng. Chem.*, **33**, 270 (2016).
5. J. Zhou, F. Gao, T. Jiao, R. Xing, L. Zhang, Q. Zhang and Q. Peng, *Colloids Surf., A*, **A 545**, 60 (2018).
6. H. Gupta and P. R. Gogate, *Ultrason. Sonochem.*, **30**, 113 (2016).
7. A. A. Taha, M. A. Shreadah, H. F. Heiba and A. M. Ahmed, *Asia-Pac. J. Chem. Eng.*, **12**(2), 292 (2017).
8. L. Ma, Q. Chen, J. Zhu, Y. Xi, H. He, R. Zhu and G. A. Ayoko, *Chem. Eng. J.*, **283**, 880 (2016).
9. R. Ahmad and A. Mirza, *J. Cleaner Prod.*, **186**, 342 (2018).
10. G. Lofrano, M. Carotenuto, G. Libralato, R. F. Domingos, A. Markus, L. Dini, R. K. Gautam, D. Baldantoni, M. Rossi, S. K. Sharma and M. C. Chattopadhyaya, *Water Res.*, **92**, 22 (2016).
11. S. Saber-Samandari, S. Saber-Samandari, S. Heydaripour and M. Abdouss, *J. Environ. Manage.*, **166**, 457 (2016).
12. R. Guo, T. Jiao, R. Li, Y. Chen, W. Guo, L. Zhang, J. Zhou, Q. Zhang and Q. Peng, *ACS Sustainable Chem. Eng.*, **6**, 1279 (2018).
13. Y. Liu, C. Hou, T. Jiao, J. Song, X. Zhang, R. Xing, J. Zhou, L. Zhang and Q. Peng, *Nanomaterials*, **8**, 35 (2018).
14. K. Li, T. Jiao, R. Xing, G. Zou, J. Zhou, L. Zhang and Q. Peng, *Sci. China Mater.*, **61**(5), 728 (2018).
15. A. A Taha, M. A. Shreadah, A. M. Ahmed and H. F. Heiba, *J. Environ. Chem. Eng.*, **4**(1) 1166 (2016).
16. S. Amirnia, M. B. Ray and A. Margaritis, *Chem. Eng. J.*, **287**, 755 (2016).
17. J. C. Moreno-Piraján and L. Giraldo, *J. Anal. Appl. Pyrolysis*, **90**(1), 42 (2011).
18. S. Agarwal, I. Tyagi, V. K. Gupta, F. Golbaz, A. N. Golikand and O. Moradi, *J. Mol. Liq.*, **218**, 494 (2016).
19. Y. Li, B. Xia, Q. Zhao, F. Liu, P. Zhang, Q. Du and Y. Xia, *J. Environ. Sci.*, **23**(3), 404 (2011).
20. R. Ahmad and A. Mirza, *Groundwater for Sustainable Develop-*

ment, **4**, 57 (2017).
21. S. Rahimi, R. M. Moattari, L. Rajabi and A. A. Derakhshan, *Colloids Surf., A*, **484**, 216 (2015).
22. Q. Cheng, Q. Huang, S. Khan, Y. Liu, Z. Liao, G. Li and Y. S. Ok, *Ecol. Eng.*, **87**, 240 (2016).
23. M. R. Lasheen, I. Y. El-Sherif, M. E. Tawfik, S. T. El-Wakeel and M. F. El-Shahat, *Mater. Res. Bull.*, **80**, 344 (2016).
24. X. H. Zhao, F. P. Jiao, J. G. Yu, Y. Xi, X. Y. Jiang and X. Q. Chen, *Colloids Surf., A*, **476**, 35 (2015).
25. A. Olgun and N. Atar, *J. Ind. Eng. Chem.*, **18**(5), 1751 (2012).
26. R. Sudha, K. Srinivasan and P. Premkumar, *Ecotoxicol. Environ. Saf.*, **117**, 115 (2015).
27. N. Arancibia-Miranda, S. E. Baltazar, A. García, D. Muñoz-Lira, P. Sepúlveda, M. A. Rubio and D. Altbir, *J. Hazard. Mater.*, **301**, 371 (2016).
28. J. Rahchamani, H. Z. Mousavi and M. Behzad, *Desalination*, **267**, 256 (2011).
29. Z. Sareban and V. Javanbakht, *Korean J. Chem. Eng.,* **34**(11), 2886 (2017).
30. A. Olgun and N. Atar, *Chem. Eng. J.*, **167**(1), 140 (2011).
31. R. Foroutan, R. Mohammadi and B. Ramavandi, *Korean J. Chem. Eng.*, **35**(1), 234 (2018).